A&A 396, 439–448 (2002)
DOI: 10.1051/0004-6361:20021389

Astronomy & Astrophysics

Infrared spectroscopy around 4 μm of Seyfert 2 galaxies: Obscured broad line regions and coronal lines⋆

D. Lutz[1], R. Maiolino[2], A. F. M. Moorwood[3], H. Netzer[4], S. J. Wagner[5], E. Sturm[1], and R. Genzel[1]

[1] Max-Planck-Institut für extraterrestrische Physik, Postfach 1312, 85741 Garching, Germany
e-mail: lutz@mpe.mpg.de, sturm@mpe.mpg.de, genzel@mpe.mpg.de
[2] Osservatorio Astrofisico di Arcetri, Largo Enrico Fermi 5, 50125 Firenze, Italy
e-mail: maiolino@arcetri.astro.it
[3] European Southern Observatory, Karl-Schwarzschild-Straße 2, 85748 Garching, Germany
e-mail: amoor@eso.org
[4] School of Physics and Astronomy and The Wise Observatory, Tel Aviv University, Tel Aviv 69978, Israel
e-mail: netzer@wise.tau.ac.il
[5] Landessternwarte, Königstuhl, 69117 Heidelberg, Germany
e-mail: S.Wagner@lsw.uni-heidelberg.de

Received 1 July 2002 / Accepted 20 September 2002

Abstract. The state of the matter that is obscuring a small circumnuclear region in active galactic nuclei can be probed by observations of its broad emission lines. Infrared lines are particularly useful since they penetrate significant columns of obscuring matter, the properties of which can be constrained by comparing infrared and X-ray obscuration. We report on new 4 μm spectroscopy with ISAAC at the ESO VLT of a sample of 12 Seyfert 2 galaxies, probing for broad components to the Brackett α 4.05 μm hydrogen recombination line. Broad components are observed in 3 to 4 objects. All objects with a broad component exhibit relatively low X-ray obscuring columns, and our results are consistent with a Galactic ratio of 4 μm obscuration to the BLR and X-ray column. In combination with observations of a *non*-Galactic ratio of *visual* obscuration of BLRs and X-ray obscuring column in Seyferts, and interpreted in a unified AGN scheme, this result can be reconciled with two interpretations. Either the properties of dust near the AGN are modified towards larger grains, for example through coagulation, in a way that significantly flattens the optical/IR extinction curve, or the ratio of dust obscuration to X-ray column varies for different viewing angles with respect to the axis of symmetry of the putative torus. Our spectra also provide a survey of emission in the [Si IX] 3.94 μm coronal line, finding variation by an order of magnitude in its ratio to Brα. The first extragalactic detection of the [Ca VII] 4.09 μm and [Ca V] 4.16 μm coronal lines is reported in the spectrum of the Circinus galaxy.

Key words. galaxies: active – galaxies: Seyfert – galaxies: ISM

1. Introduction

Unified scenarios have been highly successful in explaining several aspects of the AGN phenomenon, by assuming that different manifestations of the AGN phenomenon correspond to similar objects viewed from different directions. The detection in polarized light of broad emission lines in Seyfert 2 galaxies (Antonucci & Miller 1985; Antonucci 1993) has been central to the development of these scenarios. Subsequently, spectropolarimetry has become the prime tool for detecting hidden broad lines in larger samples (e.g., Miller & Goodrich 1990; Tran et al. 1992; Young et al. 1996; Heisler et al. 1997; Moran et al. 2000; Lumsden et al. 2001; Tran 2001). X-ray spectroscopy has been the second key observation, finding Seyfert 2s on average much more highly obscured than Seyfert 1s and quantitatively establishing the absorbing column densities in neutral and "warm", i.e. highly ionized material (e.g., Turner et al. 1997; Bassani et al. 1999). Still, relatively little is known about the actual distribution and physical state of the material obscuring the central engine of Seyfert 2 galaxies from our view. Is it in the form of a compact parsec scale torus (Krolik & Begelman 1986)? Or does obscuration on scales of tens or hundreds of parsec play a significant role (e.g. Maiolino & Rieke 1995; Malkan et al. 1998)? Mass arguments suggest that at least the Compton-thick absorbers are on scales of tens of parsecs or less (Risaliti et al. 1999), but lower column components are more difficult to constrain. Do outflows contribute to forming the obscuration (e.g. Königl & Kartje 1994; Elvis 2000)? How does the state of the obscuring matter differ from the interstellar medium in a normal galaxy, given the extreme conditions close

Send offprint requests to: D. Lutz,
e-mail: lutz@mpe.mpg.de

⋆ Based on observations collected at the European Southern Observatory, Chile (65.P-0272).

to a powerful AGN? High obscuring columns can be explained by different scenarios, and the warm dust emission seen in the mid-infrared cannot uniquely distinguish between compact and more extended configurations either (e.g., Pier & Krolik 1992; Efstathiou et al. 1995; Granato et al. 1997).

One way to address some of these issues is to study the obscuration of the central engine in wavelength ranges that are *partially* transparent at the column densities of interest, and compare the results. Of particular value are X-rays and the infrared range, but care has to be taken to compare obscuration towards similar regions. Narrow Line Region (NLR) emission and mid-infrared dust emission probe regions that are much larger than the central X-ray source. Therefore, their obscuration may involve different foreground material, and cannot be compared directly to X-ray results. In contrast, reverberation mapping results show the Broad Line Region (BLR) to be well below a parsec in size (Netzer 1990), allowing a meaningful comparison of BLR and X-ray obscuration, by material that might be found in both parsec-scale and larger regions. Our goal is to constrain infrared obscuration, and thus the state of the obscuring matter by the detection or nondetection of infrared BLRs in Seyfert 2s of various X-ray obscuring columns. Recently, Maiolino et al. (2001a) have compared visual and X-ray obscuration in Seyferts, finding large deviations from standard Galactic values. In many objects, the ratio of reddening E_{B-V} and X-ray column $N_{\rm H}$ is low by about an order of magnitude compared to the Galactic value. These results provide additional motivation to explore the relation between infrared and X-ray obscuration, and compare it with that in the visual.

Practical considerations drive the choice of the optimal transition for Broad Line Region searches in the infrared. Standard interstellar extinction laws have a minimum in the 3–8 μm range, then rise through the silicate features and drop again steeply beyond 30 μm. This tends to argue in favour of the longest wavelength infrared observations. However, the flux of the strongest (α) recombination lines drops approximately with the second power of wavelength, while dust continuum increases making their detection increasingly difficult. On the basis of such reasoning and of ISO spectroscopy of Brackett β, Brackett α, and Pfund α in NGC 1068, Lutz et al. (2000a) concluded that Brackett α with its fairly high line to continuum ratio and low obscuration is the most promising line for infrared BLR searches. Using sensitive instruments such as ISAAC on 8 m telescopes like the VLT, it is now possible to perform such observations and take a next step beyond earlier infrared searches for BLRs, which either focussed on lines that have a good line to continuum but still relatively high obscuration (Paβ 1.28 μm) or are suffering less extinction but are difficult to measure because of a low line-to-continuum ratio (Brγ 2.17 μm). Searches in these lines detected several broad components, but cannot probe beyond equivalent visual obscurations of 10–20 mag (e.g. Rix et al. 1990; Blanco et al. 1990; Goodrich et al. 1994; Ruiz et al. 1994; Veilleux et al. 1997; Gilli et al. 2000).

This paper is organized as follows. Section 2 discusses the observations and data analysis, Sect. 3 the result of a coronal line survey obtained from our data, Sect. 4 presents the results of the Brackett α spectroscopy including line decompositions. We discuss the results and compare to X-ray and optical work in Sect. 5 and conclude in Sect. 6.

2. Observations and data analysis

To identify suitable bright Seyfert 2 galaxies we have used the Bassani et al. (1999) sample with well-known X-ray obscuring columns. We have selected the objects that are brightest in extinction-corrected [O III] λ5007 ($>10^{-12}$ erg s^{-1} cm^{-2}), observable from Paranal (declination <20 deg), and are at $z < 0.015$ to keep Brackett α in the observable part of the atmospheric L band. Of the 23 objects in this parent sample, 12 were observed following right ascension and weather constraints during a run in March 9–11, 2001. Both the parent sample and the observed targets cover a wide range of X-ray obscuring columns. NGC 1068 was part of the parent sample and is included in our discussion, using the existing ISO data of Lutz et al. (2000a, 2000b) observed with a large $14'' \times 20''$ aperture. Due to the prominence of the central L band peak in NGC 1068 (Alonso-Herrero et al. 1998), the continuum of these data is still dominated by the central compact peak and can be analysed together with the smaller aperture ISAAC sample. For part of our sample, spectropolarimetric observations are available in the literature, directly confirming the intrinsic presence of a Broad Line Region. Table 1 lists this information, together with some basic source properties and total line fluxes measured from the spectra.

We used the ISAAC-LW medium resolution spectroscopy mode to cover a range of 3.93 to 4.17 μm at spectral resolving power ≈2500. This range was chosen because the rapid drop of atmospheric transmission makes longer wavelengths useless, and to ensure coverage of the [Si IX] 3.94μm coronal line in all spectra. While we present below results for this and other coronal lines obtained from our spectra, the primary motivation for including this line was to provide a reference, observed with the same instrument setting, for the line widths in the Narrow/Coronal Line Region. These can be used in cases where there is ambiguity between a true BLR and relatively broad NLR components. The bright and compact nuclei were acquired in the K band and centered in the $1''$ slit which was oriented north-south. Observations were done in the chopping and nodding along the slit scheme suited for thermal infrared observations. Integration times (excluding overheads) varied between 37 and 62 min per source. Our strategy was to integrate to good signal-to-noise in the narrow component of Brα. Then, nondetection of a broad component is meaningful, since in typical Seyfert 1s the broad line flux is several times brighter than the narrow line flux. In the sample of Stirpe (1990), for example, the median flux ratio of broad and narrow Hβ is 20 and the lowest ratio 7, for those 14 objects that do not exceed a luminosity of $M_{\rm V} = -22$ mag.

Data reduction followed standard procedures in Eclipse and IRAF. The wavelength calibration is based on arc spectra and on a vacuum scale. For flux calibration and correction for atmospheric absorptions, we observed both early type and G type stars. For our particular case of spectra near Brackett α with sometimes good continuum S/N, we found early type standards

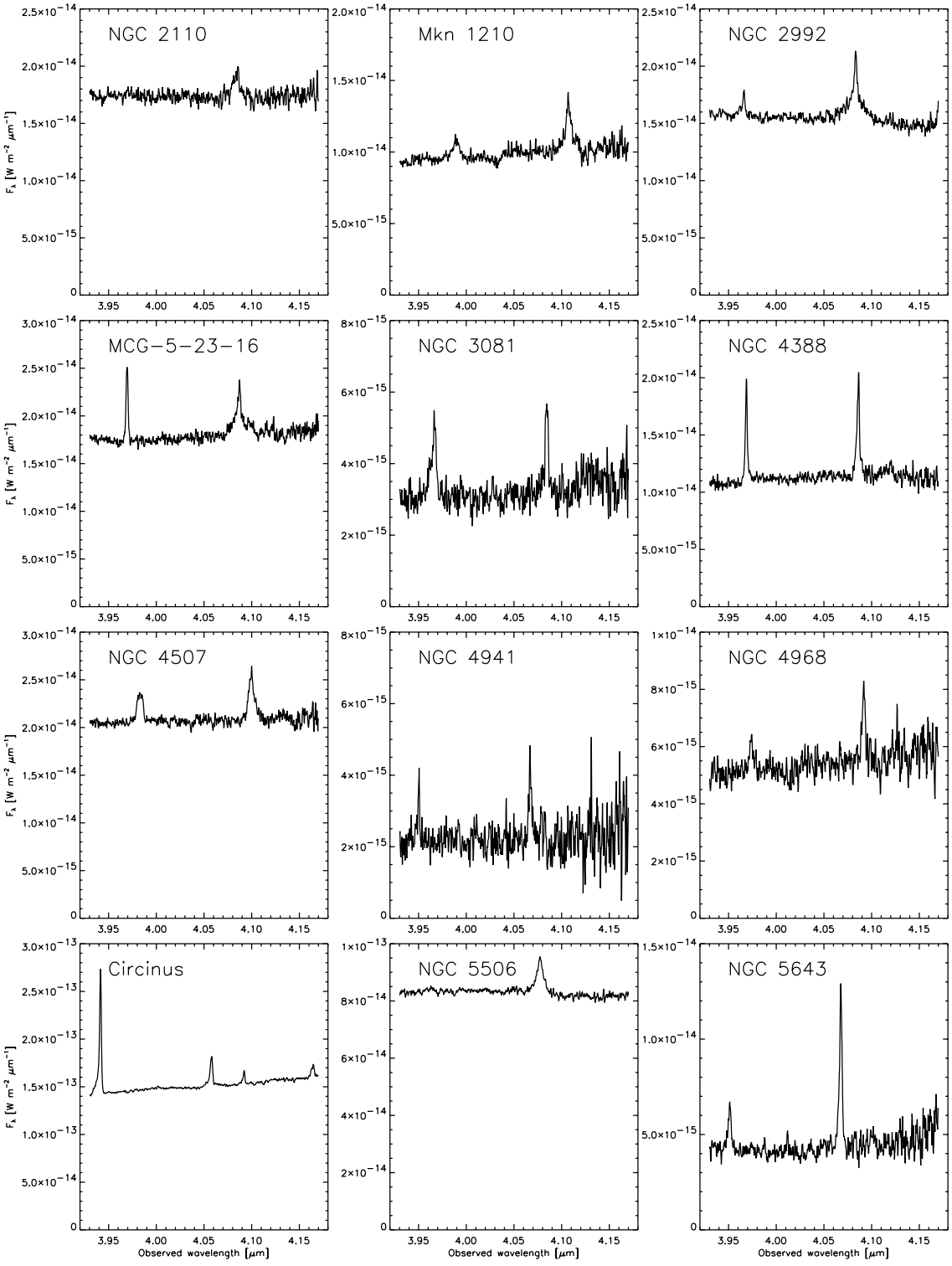

Fig. 1. ISAAC 4 μm spectra of 12 Seyfert 2 galaxies. Noise increases towards the long wavelength end because of increasing atmospheric opacity.

little suited because of difficulties to correct for their intrinsic hydrogen and helium absorption lines, and in some cases emission lines. More satisfactory correction of atmospheric absorption was achieved using early G star spectra which had first been corrected for their significant intrinsic spectral structure using the high resolution solar spectrum provided at the ESO ISAAC web pages. This solar spectrum was convolved to the appropriate resolution and slightly shifted and scaled, to give optimum cancellation of G star features when dividing a G star and solar spectrum. Since we are interested mostly in the inner region showing dust and BLR rather than NLR emission we used optimum extraction of the spectra to get the best

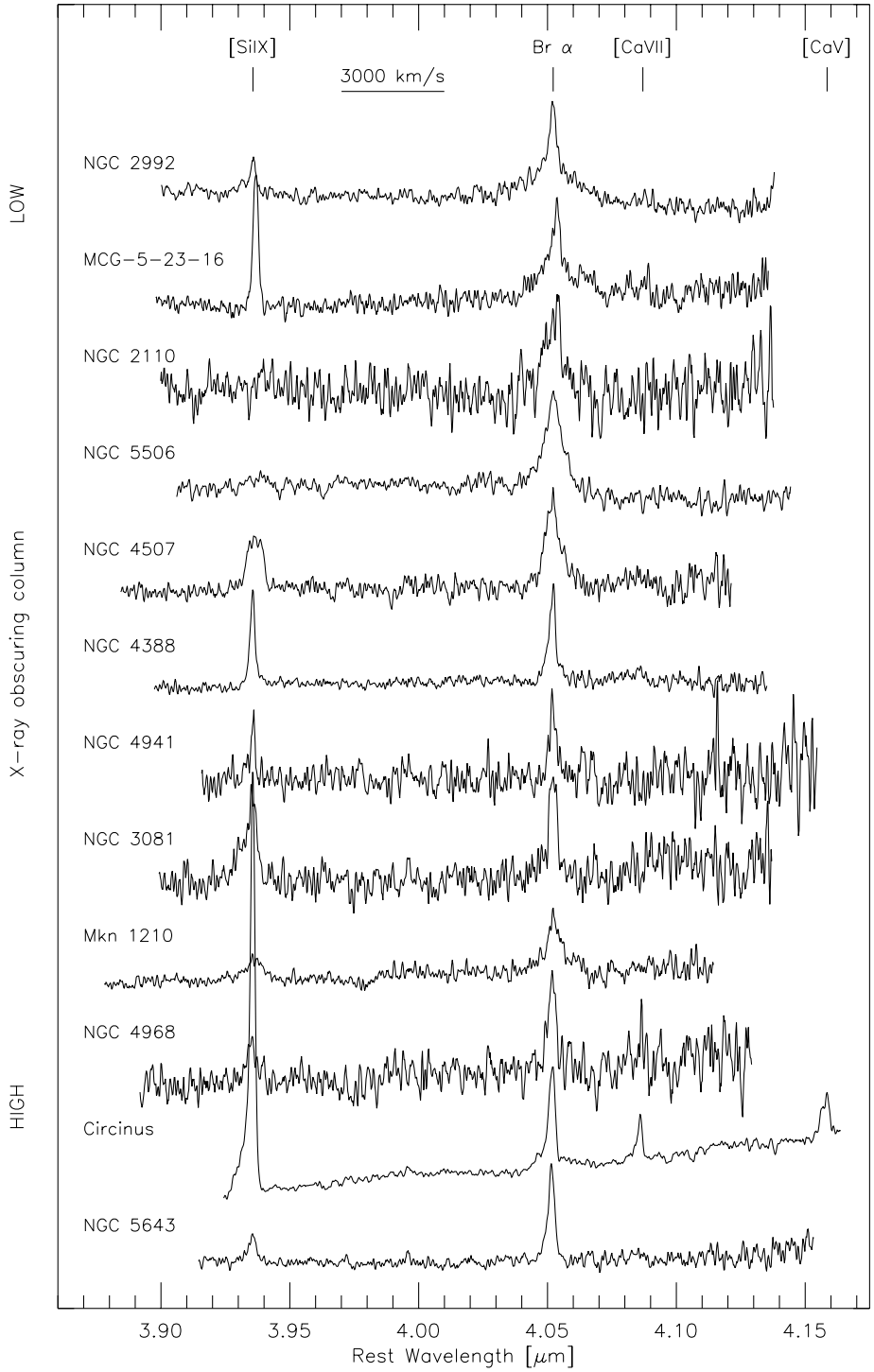

Fig. 2. Spectra sorted in order of increasing X-ray obscuring column. To facilitate comparison, the spectra have been shifted to a rest wavelength scale, continuum subtracted and scaled to the same Brα peak flux.

signal-to-noise. Effects on the NLR fluxes which in principle occur were verified to be small by inspection of the 2-D spectra and comparison of optimum extracted with directly extracted spectra. Only Circinus showed evidence for faint extended Brα emission peaking $\approx$10–15″ from the nucleus, which we did not include in the extracted spectrum. Figures 1 and 2 show the spectra, first as observed and then sorted by the X-ray obscuring column and scaled in a way facilitating comparison. Total fluxes of the coronal lines and of Brα (from direct integration of the line profiles) are listed in Table 1. Due to the narrow slit and optimum extraction scheme, they correspond to a small $\approx$1″ aperture.

3. A survey of coronal lines

The [Si IX] 3.94 μm line was first observed in an extragalactic object by Oliva et al. (1994) in the spectrum of the Circinus galaxy. It is one of the highest excitation coronal lines observed

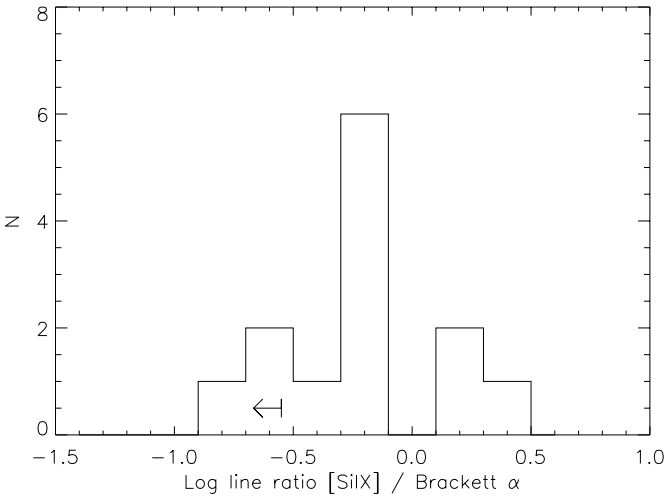

Fig. 3. Histogram for the ratio of [Si IX] 3.94 μm and the narrow component of Brα in 13 Seyfert galaxies.

in the spectra of Seyfert galaxies, with a lower ionisation potential of 303 eV. It is thus an interesting diagnostic of the coronal line region of AGN, the density of which can be constrained to be less than about 10^6 cm^{-3} using the density-sensitive ratio [Si IX] 2.58/3.94 μm (e.g. Lutz et al. 2000b). Our good signal-to-noise 4 μm spectra of 12 Seyferts significantly widen the database of observations of this line. Figure 3 shows the distribution of the ratio of [Si IX] 3.94 μm and the *narrow* (NLR) component of Brα, where we have again added NGC 1068 (Lutz et al. 2000b) to our sources. While the [Si IX] line is detected in 12 of 13 objects, the observed excitations differ strongly, with the ratio of [SiIX] and Brα varying by about an order of magnitude, similar to variations in the strength of optical coronal lines in Seyferts (e.g., Penston et al. 1984; Erkens et al. 1997).

Factors that might bias the observed ratio with respect to the intrinsic NLR one need consideration. Firstly, Brα may be contaminated by starburst emission. This effect is likely to be small in our small aperture. This can be tested on the basis of the line profiles. On the high excitation end, for Circinus both Brα and the coronal lines have similar profiles suggesting a common origin. Any starburst contribution to the observed Brα would make the intrinsic NLR excitation even higher. On the low excitation end, both [Si IX] and Brα in Mkn 1210 have similar profiles and a high $FWHM$ typical for a NLR, suggesting that both lines originate in the same region and that the low excitation is real. Another low excitation object, NGC 5643, has similar profiles for both lines but a small linewidth where a starburst contribution is difficult to discriminate kinematically. Brα cores that are narrower than for the corresponding [Si IX] line appear present in NGC 3081 and NGC 4507. These may indicate starburst contamination but could also partly reflect a NLR where lower and higher excitation species show different dynamics, as observed in some Seyferts (e.g., Appenzeller & Östreicher 1988). Secondly, underestimating the BLR contribution in a composite broad/narrow Brα profile leads to an underestimate of the [Si IX] to narrow Brα ratio. In light of the Brα profiles and their decomposition discussed in Sect. 4, such decomposition uncertainties might affect NGC 2110 and NGC 5506, which indeed are near the low end of the observed [Si IX] to narrow Brα range. Finally, excitation gradients in the NLR may bias small aperture measurements like ours towards higher excitation. For the extensively observed Circinus galaxy, comparison to larger aperture and integral field measurements of coronal lines (Oliva et al. 1994; Maiolino et al. 1998) suggests the possible effect to be less than a factor 2.

We conclude that these effects do not dominate the [Si IX]/Brα spread of about an order of magnitude among the objects of our sample. We also computed simple CLOUDY photoionization models for the "table power law" continuum implemented in CLOUDY and varying ionization parameter, showing that already modest variations of $\Delta(\log U) \sim 0.3$ near $\log U = -2$ can change [Si IX]/Brα by an order of magnitude. The observed [Si IX] flux is hence a good qualitative indicator for the presence of an AGN, but a relatively poor quantitative indicator of the AGN luminosity, due to the considerable variations of observed excitation.

Two more coronal lines are detected for the first time to our knowledge in the spectrum of an extragalactic source: [CaVII] 4.09 μm and [CaV] 4.16 μm in the spectrum of the Circinus galaxy, at wavelengths in agreement with the ones inferred by Feuchtgruber et al. (2001) from observation of the planetary nebulae NGC 6302 and NGC 7027. Like [Si IX] and Brα, they show a distinct blue asymmetry, the blue wing extending out to $\approx$800 km s^{-1}. A hint of the [Ca VII] line is seen in other high excitation spectra (NGC 4388, MCG-5-23-16) but at low significance. The rest wavelength of [Ca V] is covered by our spectra for Circinus only. Detection of these lines (lower ionisation potentials 109 and 67 eV) confirms again the unique suitability of the Circinus galaxy for coronal line studies due to its brightness, high excitation, and narrow line widths.

Observations of infrared fine-structure and coronal lines can also help elucidating the role of dust in forming the line asymmetries and shifts that are frequently observed in optical coronal lines (e.g., Erkens et al. 1997). For the prototypical Seyferts NGC 1068 and NGC 4151, these issues are discussed on the basis of ISO data by Lutz et al. (2000b) and Sturm et al. (1999). They observe some of the differences between optical and infrared lines that are expected for a moderate amount of dust in the NLR, but also find remaining asymmetries and shifts in the infrared that must either reflect intrinsic asymmetry of the NLR, or an optically extremely thick absorber that suppresses even infrared lines. We list in Table 2 the velocity offsets of narrow Brα and [Si IX] with respect to the radial velocity of Table 1 (from NED). As expected for our resolving power which is relatively low for detailed NLR profile studies, both lines are consistent with the literature radial velocity in most objects. The significant blueshift of high excitation lines in NGC 1068 has been discussed in detail by Lutz et al. (2000b). In MCG-5-23-16, both lines are redshifted by $\sim$80 km s^{-1}, possibly indicating an inaccuracy of the (optical-based) NED redshift. NGC 3081 appears to be a case like NGC 1068, with blueshift and asymmetry of the coronal line persisting in the infrared. An interesting case deserving further study is NGC 4507, where a redshift of the coronal line with respect to Brα is suggested.

Table 1. Source properties and integrated line fluxes. Heliocentric redshifts are from NED, extinction corrected [O III] fluxes from Bassani et al. (1999). X-ray obscuring columns N_H are from Bassani et al. (1999) except for Circinus (Matt et al. 1999).

Source	cz	[O III]	N_H	BLR in polarized light?	[Si IX]	Brα	[Ca VII]	[Ca V]
	km s^{-1}	10^{-14} W m^{-2}	10^{20} cm^{-2}			10^{-20} W m^{-2}		
NGC 2992	2311	0.680	69	yes (Lumsden et al. 2002)	873	6650		
MCG-5-23-16	2482	0.409	162	yes (Lumsden et al. 2002)	2150	5010	?	
NGC 2110	2335	0.321	289		<500	2110		
NGC 5506	1853	0.600	340	? (Tran 2001, Young et al. 1996)	1000:	11 700		
NGC 4507	3538	0.158	2920	yes (Moran et al. 2000)	2380	3650		
NGC 4388	2524	0.374	4200	yes (Young et al. 1996)	2530	3220	?	
NGC 4941	1108	0.355	4500	no (Moran et al. 2000)	455	804		
NGC 3081	2385	0.215	6600	yes (Moran et al. 2000)	1500	1120		
Mkn 1210	4046	0.482	$>10^4$	yes (Tran et al. 1992)	1230	2680		
NGC 4968	2957	1.116	$>10^4$		667	1060		
Circinus	449	6.970	$4\,10^4$	yes (Oliva et al. 1998)	37 700	13 900	4040	4610
NGC 5643	1199	0.694	$>10^5$	no (Moran et al. 2000)	870	2920		
NGC 1068	1137	15.86	$>10^5$	yes (Antonucci & Miller 85)	54 000	69 000		

Table 2. Kinematic data and Brα line decompositions from Gaussian fits. For objects without BLR detection, the $FWHM$ of a fit with a single Gaussian is given. Total fluxes from the fits may deviate from the values in Table 1 which are based on a direct integration of the profile. Δv describes the shift of the Gaussian fitted (narrow) line centroid with respect to the galaxy's radial velocity as listed in Table 1.

Source	$FWHM$ (b)	$FWHM$ (n)	Δv (n)	Flux (b)	Flux (n)	$FHWM$ [Si IX]	Δv [Si IX]
	km s^{-1}	km s^{-1}	km s^{-1}	10^{-20} W m^{-2}		km s^{-1}	km s^{-1}
NGC 2992	1850	230	−23	5370	1300	240	−14
MCG-5-23-16	1450	230	+84	3930	1110	190	+77
NGC 2110		618	−20	<3100			
NGC 5506	1217	fixed: 460	+39	7150	5260	640:	+150:
NGC 4507		540	−13	<4000		520	+74
NGC 4388		260	−22	<3100		190	−5
NGC 4941		260	+0	<1600		130	+16
NGC 3081		260	−16	<2300		550	−89
Mkn 1210		570	−1	<3900		670	+16
NGC 4968		270	−26	<2300		400	−31
Circinus		240	−26	<20000		170	+6
NGC 5643		250	−35	<3100		290	+4
NGC 1068		640	−27	<80000		590	−187

4. Results of the Brackett α spectroscopy

In clear cases like NGC 2992, the broad component of Brackett α is easily discriminated from the narrow component. At intermediate line widths, the situation is sometimes ambiguous, however. It is not obvious whether a line originates in a true BLR of dense clouds close to the AGN, or whether it represents an unusually wide NLR profile that is seen similarly in the forbidden and coronal lines (see the example of NGC 1068; e.g. Lutz et al. 2000a, 2000b). We hence applied the definition of a broad line as "a component of Brackett α with $FWHM$ around 1000 km s^{-1} or more that is not seen in the forbidden or coronal lines", and used the [Si IX] line as reference. Table 2 summarizes our decompositions from Gaussian fits. In cases where we do not detect a broad component, we quote an approximate upper limit for its flux determined under the assumption of a representative value of 3000 km s^{-1} $FWHM$ for the BLR (e.g. Osterbrock 1977). One should note, however, that the spectral coverage of the data makes detection of very broad ($FWHM$ 10 000 km s^{-1}) lines difficult even if the flux were larger.

A number of objects deserve an individual justification of our decision to identify a line as originating in a BLR or not, also to indicate remaining ambiguities. The Brackett α line of Mkn 1210, for example, can be plausibly decomposed into a broad and a narrow component. We decided against a BLR interpretation, however, because the [Si IX] line shows wide wings as well, the two profiles being indistinguishable within the S/N limitations. This argues against the interpretation of Veilleux et al. (1997) who considered Mkn 1210 a BLR detection (but see caveats in their appendix). Their [Fe II] and Paschen β profiles are very similar to our [Si IX] and Brackett α profiles, while we do not find evidence for the $FWHM$ 3000 km s^{-1} component possibly seen in their Brackett γ data.

Another complex case is NGC 5506 where a broad component to Paschen β has been reported (Blanco et al. 1990; Rix et al. 1990). Goodrich et al. (1994) and Veilleux et al. (1997) confirm the larger width of this infrared line compared to optical lines but, on the basis of a similar [Fe II] profile, ascribe this effect to a moderately broad but obscured component of the NLR. Our profile of Brackett α is relatively broad but not obviously the sum of a narrow and a broad line. Comparison to

[Si IX] does not help in this case because of its weak and uncertain detection in NGC 5506, making the measured $FWHM$ highly uncertain. We hence compared the Brackett α profile with ISO spectroscopy of the [O IV] 26 μm forbidden line in this object (Sturm et al. 2002) which is able to penetrate large obscuring columns. We fixed the NLR $FWHM$ for the ISAAC spectrum to the value of 460 km s^{-1} which is based on the $FWHM$ measured from a Gaussian fit to [O IV], corrected for the resolution difference of ISO-SWS and ISAAC. Adopting this NLR line width we obtain a residual BLR component with $FWHM$ similar to the one of Blanco et al. (1990) but significantly lower than the value reported by Rix et al. (1990), most likely reflecting line profile decomposition uncertainties of the various datasets. We also checked for differences between the fine-structure line $FWHM$ (Sturm et al. 2002) and the optical $FWHM$ of Veilleux (1991a, 1991b) that would be expected if extinction within the NLR dominates the profiles. No significant differences were found when convolving the optical data to the lower resolution and consistently measuring the $FWHM$ by gaussfits. On the basis of an O I fluorescence line and of J band [Fe II] transitions, Nagar et al. (2002) argue that NGC 5506 is an obscured Narrow Line Seyfert 1, consistent with our decomposition which ascribes most of Brα to a fairly narrow BLR.

The most uncertain case is NGC 2110 with its moderately wide Brackett α line. The nondetection of [Si IX] and the absence of ISO spectroscopy makes a direct comparison to the forbidden lines impossible. Evidence on possible broad components to Paschen β is mixed (Rix et al. 1990; Veilleux et al. 1997). We have listed this case as a narrow line, on the basis of the similarity of the Brackett α line width with that of [Fe II] (Veilleux et al. 1997). We will include this object as uncertain when discussing the sample statistics below.

Figure 4 summarizes the detections and limits on broad components of Brackett α in our sample objects. Relatively few broad line regions are found – only 3 to 4 out of 13 (considering the uncertain case of NGC 2110). For the nondetections, limits for broad Brα components are of the order 1 to 2 times the narrow Brα flux. Assuming intrinsic presence of a BLR, as confirmed by spectropolarimetry for most of the objects, and an intrinsic broad to narrow line ratio 20 equal to the median of the Stirpe (1990) $M_V < -22$ Seyfert 1s, these limits imply an obscuration of broad Brackett α of $\approx$3 mag. For a Galactic extinction curve, this corresponds to an equivalent visual extinction of more than 50 mag. For $A_{4.05}/A_V = 0.035$ (Draine 1989) the equivalent visual extinction would be 86 mag, for $A_{4.05}/A_V = 0.051$ (Lutz 1999) 59 mag. Assuming a canonical conversion factor from visual extinction to X-ray obscuring column of $N_H/A_V = 1.79 \times 10^{21}$ cm^{-2} (e.g. Predehl & Schmitt 1995), broad components to Brackett α should remain visible up to X-ray obscuring columns of about 10^{23} cm^{-2}. The fact that all our BLR detections are below this limit is thus consistent with a Galactic value of the ratio of 4 μm obscuration to X-ray column.

At this point, a comparison to the factors determining the detectability of Seyfert 2 BLRs in polarized light is in place. The dominant factor for BLR detectability in polarized light is AGN luminosity, probably both through the corresponding variation of host galaxy dilution and through a varying size of the scattering region (e.g. Alexander 2001; Lumsden et al. 2001; Lumsden & Alexander 2001). The BLR detectability in polarized light one modestly depends on the X-ray column (Lumsden et al. 2001), there are BLR detections up to the highest X-ray columns. Since most of our objects do have detections of the BLR in polarized light (Table 1), and were selected to be bright in [O III], we believe that the effect of AGN luminosity and host dilution on the BLR detectability in our spectroscopy is less important than the effect of obscuration.

5. Discussion

Our observations have resulted in the detection of broad line regions in about one quarter of the Seyfert 2 sample studied. This fraction is similar to the one reported at shorter near-infrared wavelengths by Veilleux et al. (1997). Small numbers and the difficulties discussed above to ascribe moderately broad profiles for some of the objects to a BLR or the NLR limit a detailed intercomparison of these fractions. It is clear, however, that the detection rate at the wavelength of 4 μm which samples columns up to 10^{23} cm^{-2} (for a Galactic extinction curve) is not much higher than in the shorter wavelength studies which penetrate 3 to 5 times smaller columns. This cannot reflect intrinsic absence of BLRs since they are detected through spectropolarimetry in the majority of the objects with 4 μm BLR nondetections. The majority of Seyfert 2s thus still has considerable BLR obscuration at 4 μm. This finding is still consistent with most popular models of dust around AGN, though being close to constraining the ones that predict the most modest obscurations (e.g., Granato et al. 1997). It is already exceeding the modest obscurations (A_V up to a few tens) predicted for most polar angles ($\theta < 80$ deg) in the disk wind model of Königl & Kartje (1994).

The high 4 μm obscuration and the consistency with a Galactic extinction curve raise an apparent conflict with the abnormally low ratios of *visual* reddening E_{B-V} and X-ray column in luminous AGN, as summarized by Maiolino et al. (2001a). Comparing reddening E_{B-V} towards the BLR as measured from optical spectra with X-ray N_H, they find this ratio to be 3 to 100 times lower than Galactic for most of the objects in their sample. Based on other evidence, they suggest the ratio of visual extinction A_V and N_H to be lower than Galactic as well, for several classes of AGN. Simply lowering the dust content in the absorber and releasing the metals into the gas does not solve this discrepancy of about an order of magnitude. In addition to other effects discussed by Maiolino et al. (2001b), a low dust-to-gas ratio should result in the detection of broad Brackett α lines at X-ray columns approaching 10^{24} cm^{-2}, but none are observed in our sample.

Geometry effects may play a role since the samples are different. Maiolino et al. (2001a) mainly observed Seyfert 1s, Quasars and intermediate Seyferts, since optical detection of a BLR was pre-requisite for their analysis. Here, we analyze intermediate and type 2 objects, that is ones viewed more "edge-on" in the picture of a central torus. If, as not implausible, dust were preferentially modified or destroyed along the opening of the torus, then different lines of sight probe different dust

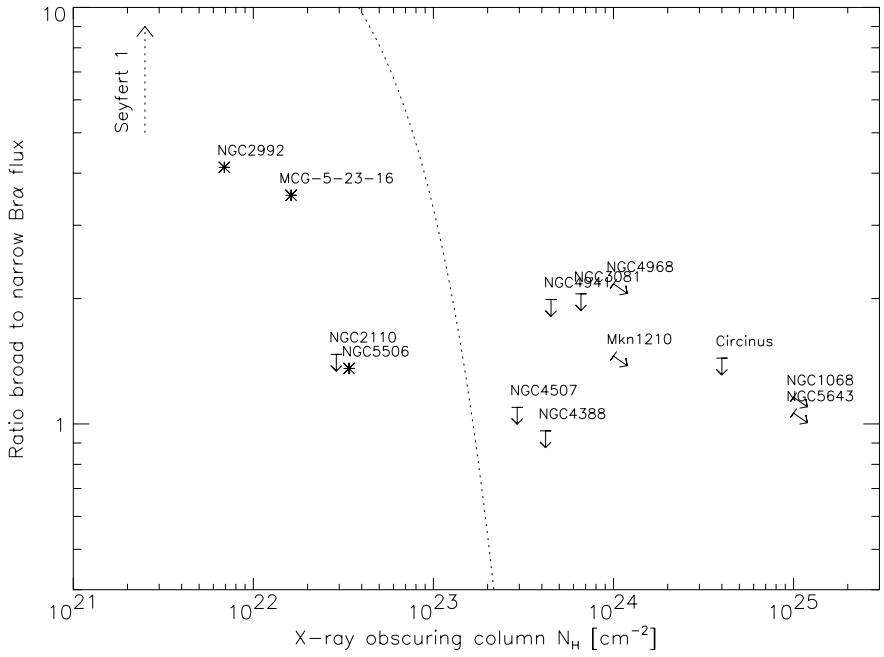

Fig. 4. Flux ratio of broad and narrow components of Brackett α, as a function of X-ray obscuring column. For BLR nondetections we plot the ratio of an upper limit for a *FWHM* 3000 km s^{-1} BLR to the total observed (= narrow) Brackett α flux. As qualitatively indicated, Seyfert 1 galaxies would populate the upper left of this diagram and even larger ratios of broad and narrow flux (e.g., Stirpe 1990, median 20 in that sample). The curved dotted line indicates the location of an object having an intrinsic broad to narrow line ratio of 20, with the broad component increasingly obscured by dust with a Galactic ratio of infrared to X-ray obscuration. Changing adopted dust properties would move this line horizontally, changing the adopted intrinsic ratio would move the line vertically.

properties. The modified dust may be found detached in the opening of the torus, or associated with the walls. Similarly, the dusty wind model of Königl & Kartje (1994) provides a geometry where dust-free gas is surrounded by dusty gas but, as noted above, predicts relatively low obscuration. Another geometric option is that "normal" dust on large scales (100 pc or more) contributes to the obscuration, as well as "modified" circumnuclear dust, the two covering different directions. This geometry is similar to the scenario proposed by Maiolino & Rieke (1995) for the RSA Seyferts, but with the difficulty that they invoke the likely more "normal" large scale dust to create the obscuration of intermediate Seyferts. This conflicts with observations that intermediate Seyferts do show anomalous relations of optical and X-ray columns (Maiolino et al. 2001a). This is not consistent with "normal" galactic dust, unless one postulates that there is a spatial separation between X-ray absorber (dust-free and close to the nucleus) and normal dust optical absorption on large scale (Weingartner & Murray 2002).

The seemingly discrepant optical and 4 μm results are, however, also consistent with the preferred interpretation of Maiolino et al. (2001b) for the results of Maiolino et al. (2001a). If dust in the dense circumnuclear regions of AGN is dominated by large grains, as proposed by Laor & Draine (1993) and by Maiolino et al. (2001b), the net effect on the extinction curve will be mainly a reduction at short wavelengths, but much less change in the infrared. This is illustrated in the top panel of Fig. 5, where the Galactic "standard" extinction curve is compared with an extinction curve due to a grain distribution biased in favor of large sizes[1]. This effect would explain both the mismatch between optical extinction and gaseous column measured in the X-rays (discussed in Maiolino et al. 2001a) and the agreement between IR extinction and X-ray absorption found in this paper.

The "large grains" curve has a turnover at about 2–3 μm (at variance with the "Galactic" curve) which is nicely probed by the three infrared hydrogen lines Paβ, Brγ and Brα. In case of (screen) absorption, the deviation of the line ratios from the intrinsic case B depends significantly on the extinction curve, this is shown in the lower panel of Fig. 5. For two of the sources showing broad Brα, namely NGC 2992 and MCG-5-23-16, there are measurements in the literature for the broad components of Paβ and Brγ (Gilli et al. 2000; Veilleux et al. 1997), which allow to locate these objects in the lower panel of Fig. 5. The location of NGC 2992 is inconsistent with the Galactic extinction curve, but fully consistent with the "large grains" scenario. For MCG-5-23-16 the location is not even consistent with the Galactic extinction, because of the very low Brα/Paβ ratio. This might be due to variability of the BLR, since Brα (this paper) and Paβ (Veilleux et al. 1997) were not measured simultaneously but with a time lag of 9 years. This point of view is strengthened by the data of

[1] More specifically, the distribution of grain sizes has been modelled with $n \propto a^{-\beta}$, $\beta = 2.5$, $a_{\rm min} = 0.005$ μm, $a_{\rm max} = 1$ μm, among those suggested by Laor & Draine (1993) and by Maiolino et al. (2001b), at variance with the "standard" distribution for the Galactic dust, where $\beta = 3.5$, $a_{\rm min} = 0.005$ μm, $a_{\rm max} = 0.25$ μm. See also Maiolino et al. (2001b).

Blanco et al. (1990) who, another 3 years earlier, measured a 4 times lower broad Paβ flux. The caveat of variability might also apply to NGC 2992, though here the measurements were much closer in time (2 years) and the data from Gilli et al. (2000) have higher accuracy. Additional, simultaneous measurements of the broad components of the infrared hydrogen lines are required to unambiguously test the "large grains" scenario.

We note that a population of large grains in the dense circumnuclear regions of AGN is not an ad hoc requirement, but in line with the flattened extinction curves in Galactic dense molecular clouds (e.g. Cardelli et al. 1989) which are ascribed to grain coagulation. However, grain growth may yield the formation of complex fluffy aggregrates (e.g., Dominik & Tielens 1997) rather than the simply larger but spherical grains, which are assumed in the simplified model of Fig. 5. Finally, a dust distribution biased for large grains may also come from the preferential destruction of small grains by sublimation or sputtering in the circumnuclear region of AGN. Depending on the mechanism producing a dust distribution that is biased toward large grains, the *absolute* extinction $A_{4\ \mu\mathrm{m}}/N_{\mathrm{H}}$ may differ. In case of destruction of small grains it will be below but similar to the Galactic value, while for coagulation at a fixed dust mass it will rise above the Galactic value. Figure 4 is consistent with modest deviations in either direction.

The current data do not allow to discriminate between the "geometrical" and the "large grains" scenario. Both are plausible within the unified scenario for AGN. A better understanding, at least for the intermediate type Seyferts with moderate A_{V} could be gained through simultaneous observations of the main optical to 4 μm recombination lines, in order to directly trace the flattening of the extinction curve expected in the large grain scenario. Line ratios formed by the broad components of Brackett α, Brackett γ, and Paschen β (Fig. 5) are better suited than a similar diagram invoking the Balmer decrement, because of the reduced susceptibility to departures from case B (e.g. Netzer 1990 and references therein). While Fig. 5 proposes a direct test for the presence of large grains, future quasi-simultaneous and accurately calibrated data will be needed for a conclusive result.

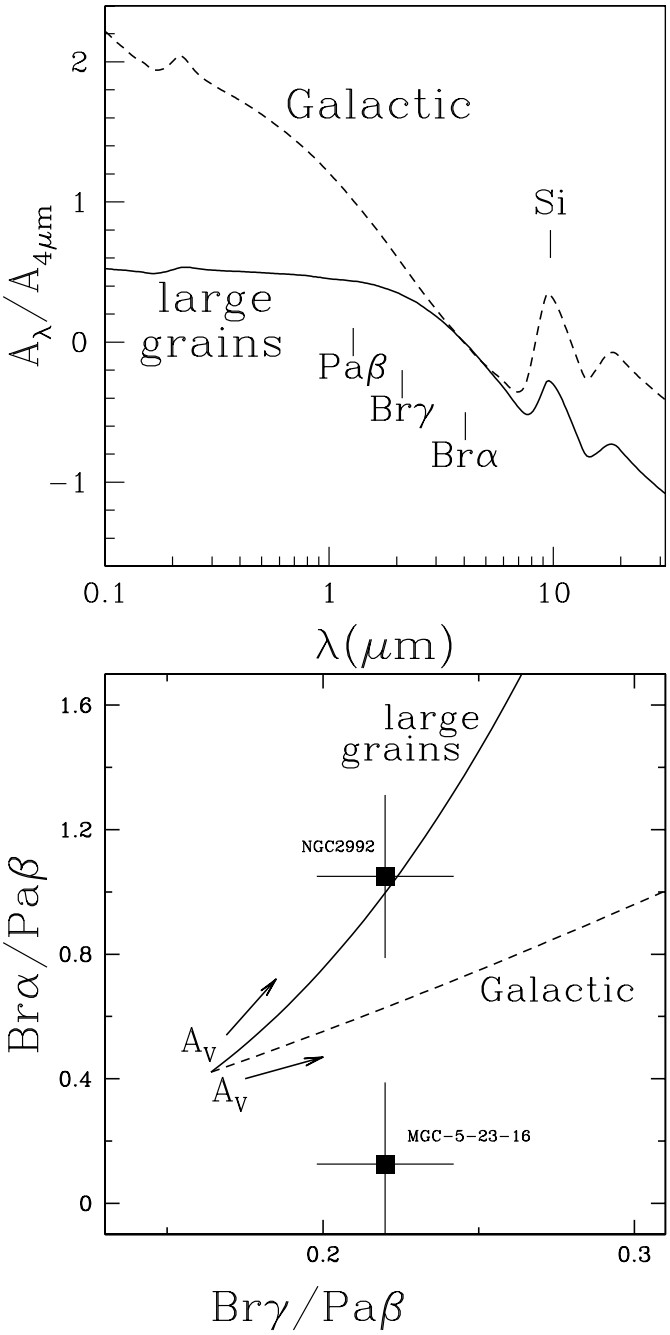

Fig. 5. Top: Changing the dust size spectrum from a standard "Galactic" one to one dominated by large grains may flatten the extinction curve in the optical and induce a knee in the near-infrared (see text for details). Bottom: Expected near-infrared broad line ratios for increasing obscuration and the two cases of standard Galactic grains and large grains. The adopted intrinsic ratios are for case B and $T_{\mathrm{e}} = 20\,000$ K, $n_{\mathrm{e}} = 10^9$ cm^{-3}. The two objects from our Brα sample for which *non-simultaneous* Paβ and Brγ data are available are indicated. Future quasi-simultaneous and accurately calibrated spectroscopy is needed to actually execute this test.

6. Conclusions

We have presented new 4 μm spectroscopy of a sample of 12 Seyfert 2 galaxies that are well-studied in the X-ray, and combine these data with previous spectroscopy of NGC 1068. The observations are designed to probe for the presence of optically obscured Broad Line Regions. The main results are:

(i) Broad components to Brackett α are detected in 3 to 4 of these 13 galaxies.

(ii) The detections and limits are consistent with a Galactic ratio of infrared and X-ray obscuring columns. This result can be reconciled with the low ratios of optical to X-ray obscuring columns observed for several AGN if either the obscuring dust consists of large grains leading to a modified extinction curve, or if variation in dustiness or dust properties exists between directions probing right through the putative torus and directions closer to its opening.

(iii) A survey of the coronal [Si IX] 3.94 μm line shows considerable variation in its ratio to Brackett α.

(iv) Two coronal lines of [Ca VII] and [Ca V] are detected for the first time in an extragalactic object, the Circinus galaxy.

Acknowledgements. We thank the Paranal staff for excellent support, Bill Vacca for discussions, and the referee for helpful comments. This work is supported by GIF grant I-551-186.07/97.

References

Alexander, D. M. 2001, MNRAS, 320, L15
Alonso-Herrero, A., Simpson, C., Ward, M. J., & Wilson, A. S. 1998, ApJ, 495, 196
Antonucci, R. R. J., & Miller, J. S. 1985, ApJ, 297, 621
Antonucci, R. R. J. 1993, ARA&A, 31, 473
Appenzeller, I., & Östreicher, R. 1988, AJ, 95, 45
Bassani, L., Dadina, M., Maiolino, R., et al. 1999, ApJS, 121, 473
Blanco, P. R., Ward, M. J., & Wright, G. S. 1990, MNRAS, 242, 4
Cardelli, J. A., Clayton, G. C., & Mathis, J. S. 1989, ApJ, 345, 245
Dominik, C., & Tielens, A. G. G. M. 1997, ApJ, 480, 647
Draine, B. T. 1989, in Proc. 22nd Eslab Symp. on Infrared Spectroscopy in Astronomy, ESA SP-290, (Noordwijk: ESA), 93
Efstathiou, A., Hough, J. H., & Young, S. 1995, MNRAS, 277, 1134
Elvis, M. 2000, ApJ, 545, 63
Erkens, U., Appenzeller, I., & Wagner, S. 1997, A&A, 323, 707
Feuchtgruber, H., Lutz, D., & Beintema, D. 2001, ApJS, 136, 221
Gilli, R., Maiolino, R., Marconi, A., et al. 2000, A&A, 355, 485
Goodrich, R. W., Veilleux, S., & Hill, G. J. 1994, ApJ, 422, 521
Granato, G. L., Danese, L., & Franceschini, A. 1997, ApJ, 486, 147
Heisler, C. A., Lumsden, S. L., & Bailey, J. A. 1997, Nature, 385, 700
Königl, A., & Kartje, J. F. 1994, ApJ, 434, 446
Krolik, J. H., & Begelman, M. 1986, ApJ, 308, L55
Laor, A., & Draine, B. 1993, ApJ, 402, 411
Lumsden, S. L., Heisler, C. A., Bailey, J. A., et al., 2001, MNRAS, 327, 459
Lumsden, S. L., & Alexander, D. M. 2001, MNRAS, 328, L32
Lutz, D. 1999, in The Universe as seen by ISO, ed. P. Cox, & M. F. Kessler, ESA-SP427, 623
Lutz, D., Genzel, R., Sturm, E., et al. 2000a, ApJ, 530, 733
Lutz, D., Sturm, E., Genzel, R., et al. 2000b, ApJ, 536, 697
Maiolino, R., & Rieke, G. H. 1995, ApJ, 454, 95
Maiolino, R., Krabbe, A., Thatte, N., & Genzel, R. 1998, ApJ, 493, 650
Maiolino, R., Marconi, A., Salvati, M., et al. 2001a, A&A, 365, 28
Maiolino, R., Marconi, A., & Oliva, E. 2001b, A&A, 365, 37
Malkan, M. A., Gorjian, V., & Tam, R. 1998, ApJS, 117, 25
Matt, G., Guainazzi, M., Maiolino, R., et al. 1999, A&A, 341, L39
Miller, J. S., & Goodrich, R. W. 1990, ApJ, 355, 456
Moran, E. C., Barth, A. J., Kay, L. E., & Filippenko, A. V. 2000, ApJ, 540, L73
Nagar, N. M., Oliva, E., Marconi, A., & Maiolino, R. 2002, A&A, 391, L21
Netzer, H. 1990, in Active Galactic Nuclei, ed. T. J. L. Courvoisier, & M. Mayor, Saas Fee Course 20 (Berlin: Springer Verlag), 57
Oliva, E., Salvati, M., Moorwood, A. F. M., & Marconi, A. 1994, A&A, 288, 457
Oliva, E., Marconi, A., Cimatti, A., & di Serego Alighieri, S. 1998, A&A, 329, L21
Osterbrock, D. E. 1977, ApJ, 215, 733
Penston, M. V., Fosbury, R. A. E., Boksenberg, A., Ward, M. J., & Wilson, A. S. 1984, MNRAS, 208, 347
Pier, E. A., & Krolik, J. H. 1992, ApJ, 401, 99
Predehl, P., & Schmitt, J. H. M. M. 1995, A&A, 293, 889
Risaliti, G., Maiolino, R., & Salvati, M. 1999, ApJ, 522, 157
Rix, H.-W., Carleton, N. P., Rieke, G., & Rieke, M. 1990, ApJ, 363, 480
Ruiz, M., Rieke, G. H., & Schmidt, G. D. 1994, ApJ, 423, 608
Stirpe, G. M. 1990, A&AS, 85, 1049
Sturm, E., Alexander, T., Lutz, D., Netzer, H., & Genzel, R. 1999, ApJ, 512, 197
Sturm, E., Lutz, D., Verma, A., et al., 2002, A&A, 393, 821
Tran, H. D., Miller, J. S., & Kay, L. E. 1992, ApJ, 397, 452
Tran, H. D. 2001, ApJ, 554, L19
Turner, T. J., George, I. M., Nandra, K. M., & Mushotzky, R. F. 1997, ApJS, 113, 23
Veilleux, S. 1991a, ApJS, 75, 357
Veilleux, S. 1991b, ApJS, 75, 383
Veilleux, S., Goodrich, R. W., & Hill, G. J. 1997, ApJ, 477, 631
Weingartner, J. C., & Murray, N. 2002, ApJ, in press [astro-ph/0208123]
Young, S., Hough, J. H., Efstathiou, A., et al. 1996, MNRAS, 281, 1206